Available online at www.sciencedirect.com
SCIENCE DIRECT
Journal of Catalysis 227 (2004) 492–501
JOURNAL OF CATALYSIS
www.elsevier.com/locate/jcat

Correlation of NO and CO_2 adsorption sites with aldehyde hydrogenation performance of sulfided Ni–Mo/Al_2O_3 catalysts

Xueqin Wang, Umit S. Ozkan *

Department of Chemical Engineering, The Ohio State University, 140 West 19th Avenue, Columbus, OH 43210, USA

Received 26 May 2004; revised 30 July 2004; accepted 7 August 2004

Available online 16 September 2004

Abstract

Hydrogenation of aldehydes over sulfided Ni–Mo/Al_2O_3 catalysts was studied using hexanal and propanal as model feed compounds. NO adsorption and CO_2 adsorption measurements, which are used to probe the coordinatively unsaturated sites (CUS) and the hydroxyl groups on the alumina surface of sulfided Mo catalysts, were found to correlate well with alcohol and heavy product formation rates, respectively. Static chemisorption measurements as well as diffuse reflectance Fourier transform infrared spectroscopy analysis were used in the quantification of the CUS and OH sites on the surface. The anion vacancies associated with Ni sites were found to have a higher intrinsic activity for hydrogenation of aldehyde to alcohol. Although CO_2 can provide some measure of the exposed alumina surface, it tends to overestimate the surface coverage since it adsorbs preferentially on more basic OH sites. Therefore, quantification of the OH groups relative to the bare alumina surface appears to provide a more accurate measure of the surface coverage, and to correlate better with the heavy product formation in aldehyde hydrogenation.

Keywords: Aldehyde hydrogenation; Sulfided Mo catalysts; NO and CO_2 adsorption; DRIFTS; Hydroxyl groups

1. Introduction

Sulfided CoMo and NiMo catalysts that are supported on Al_2O_3 have been studied extensively, especially with regard to their catalytic performance in hydrodesulfurization (HDS) and hydrodenitrogenation (HDN) reactions [1–7]. According to a widely accepted model proposed by Topsoe and co-workers, these catalysts consist of stacks of MoS_2 layers supported over alumina and the Ni or Co species are located on the edges of these stacks (i.e., CoMoS and NiMoS phases) [3,8–10].

Oxo process alcohols are a major class of organic chemicals [11]. The oxo process (i.e., hydroformylation) consists of reacting an olefin with carbon monoxide and hydrogen at elevated temperatures and pressures, in the presence of a suitable catalyst, to produce an aldehyde with a carbon number one higher than the starting olefin. Depending on the process conditions, the resulting products may be aldehydes, primary alcohols, or a mixture of the two. The product stream from the oxo process needs to be hydrogenated to convert the aldehydes to alcohols. Several different catalysts are used in industry to convert aldehydes to alcohols. Catalysts frequently used include copper chromite, molybdenum sulfide, nickel, and cobalt. Although copper chromite has excellent hydrogenation activity, it is also very sensitive to sulfur poisoning, making it difficult to use with sulfur-containing feed streams. Sulfided Ni–Mo/Al_2O_3 catalysts provide excellent hydrogenation activity while showing a high tolerance to sulfur compounds.

Although there are excellent correlations between the active sites on NiMoS/Al_2O_3 or CoMoS/Al_2O_3 catalysts and their performance in HDS and HDN reactions, the relationships between the sites and the different steps involved in aldehyde hydrogenation reactions are not well established. In addition to the anion vacancies associated with Mo or Ni centers, i.e., coordinatively unsaturated sites (CUS), the

* Corresponding author. Fax: +1 614 292 9615.
E-mail address: ozkan.1@osu.edu (U.S. Ozkan).

0021-9517/$ – see front matter
doi:10.1016/j.jcat.2004.08.009

Brønsted acid sites and different OH groups with varying levels of acidity are expected to play a role in determining the selectivity toward different products and intermediates in aldehyde hydrogenation. Characterization of active sites by adsorption of probe molecules has been successfully used in several studies. NO and CO_2 are two molecules that have been used for probing anion vacancy sites and exposed alumina sites over $NiMoS/Al_2O_3$ catalysts, respectively [12–17, and references therein]. In this article, we present the results from our studies which focused on identification of active sites over $NiMoS/Al_2O_3$ catalysts for the primary reactions involved in the aldehyde hydrogenation network, using two different linear aldehydes, hexanal and propanal, as the starting materials.

2. Experimental

Alumina-supported catalysts with different Mo and Ni loadings were prepared by wet coimpregnation of γ-Al_2O_3 with aqueous solutions of ammonium heptamolybdate and nickel nitrate. The preparation procedure was presented previously [18–20]. The catalyst compositions are reported as weight percentages of the oxide precursors, i.e., MoO_3 and NiO, following the convention commonly used in the literature. The surface area of samples used in these studies varied between 166 and 195 m^2/g, with pure alumina giving the highest surface area [20]. Prior to all reaction studies, the catalysts were sulfided in situ at 400 °C with 10% H_2S in H_2 for 10 h followed by flushing with He for 1 h at the same temperature before cooling the system to the desired reaction temperature. The reaction studies on hexanal and propanal hydrogenation were carried out in a fixed-bed reactor system, which is described in previous articles [20,21].

2.1. DRIFTS studies

Diffuse reflectance infrared Fourier transform spectroscopy (DRIFTS) experiments were performed using a Bruker IFS66 instrument equipped with DTGS and MCT (operated at 77 K) detectors and a KBr beam splitter. Catalyst was placed in a sample cup inside a Spectrotech diffuse reflectance cell equipped with KBr windows and a thermocouple mount that allowed direct measurement of the surface temperature. Spectra for each experiment were averaged over 1000 scans in the mid-IR range (400–4000 cm^{-1}) to a nominal 3 cm^{-1} resolution. After in situ pretreatment of the samples at 400 °C for 2 h in a He flow of 30 cm^3/min, the temperature was decreased to room temperature and the background spectra were taken under He flow. The adsorption process was carried out by introducing NO (5450 ppm in He) or CO_2 into the system at room temperature for 1 h. After adsorption, the system was subsequently purged for 1 h with He at a flow rate of 30 cm^3/min. Then the spectra were collected under He flow and the background spectrum was subtracted from the postadsorption spectra.

2.2. Volumetric measurement of adsorbed probe molecules

The volumetric measurements of CO_2 and NO chemisorption were performed using a Micromeritic ASAP2010 instrument. Before chemisorption measurements, the catalysts were pretreated in situ under the same conditions as those used prior to reaction in the reactor. The first adsorption isotherm was established by measuring the amount of gas adsorbed as a function of pressure. After completing the first adsorption isotherm, the system was evacuated for 1 h at 10^{-5} mm Hg. Then a second adsorption isotherm was obtained. The amount of probe molecule chemisorbed was calculated by taking the difference between the two isothermal adsorption amounts. The surface coverage of Al_2O_3 support by molybdenum species, Cs_{CO_2}, based on the amount of chemisorbed CO_2, was calculated by the expression

$$\%Cs_{CO_2} = \left[1 - \left\{n_{CO_2,cat}/(1 - m/100)\right\}/n_{CO_2,Al}\right] \times 100, \quad (1)$$

where $n_{CO_2,cat}$ and $n_{CO_2,Al}$ are the amounts of chemisorbed CO_2 per gram catalyst and Al_2O_3 support, respectively, and m is the wt% of MoO_3 loading in the oxidic catalysts.

3. Results and discussion

3.1. DRIFTS studies

DRIFT spectra of adsorbed CO_2 and NO over bare alumina support, Mo/Al_2O_3, and $Ni–Mo/Al_2O_3$ catalysts are presented in Fig. 1. The spectra are taken using a MCT detector. The support and the catalysts are sulfided prior to CO_2 and NO adsorption. The major bands of adsorbed CO_2 (Fig. 1a) are at 1650, 1440, and 1226 cm^{-1}. The observation that the intensity of these bands decreases monotonically with increasing Mo loading is consistent with earlier reports where CO_2 was found to adsorb primarily on the bare alumina sites [13,15,20]. The bands observed over the sulfided alumina are similar to those observed over the oxidized alumina surface [20,22]. The intensity of the CO_2 adsorption bands over the 20% Mo/Al_2O_3 monometallic catalyst (not shown) were found to be similar to those over 15% Mo/Al_2O_3. The intensities over the bimetallic 3% Ni–15% Mo/Al_2O_3 catalyst, however, were lower than those observed over the monometallic 15% Mo/Al_2O_3, suggesting that the presence of Ni may be enhancing the dispersion of Mo on the surface. This observation is consistent with our earlier results obtained through laser Raman and X-ray photoelectron spectroscopy studies [19].

Fig. 1b shows the NO adsorption bands over sulfided mono and bimetallic catalysts. As it is well established in the literature, NO is a selective adsorbate for probing the coordinatively unsaturated sites. The bands at 1796 and 1707 cm^{-1} are assigned to symmetrical and asymmetrical stretching vibrations of NO in the dinitrosyl complex and they grow in intensity with increased Mo loading. The bimetallic catalyst

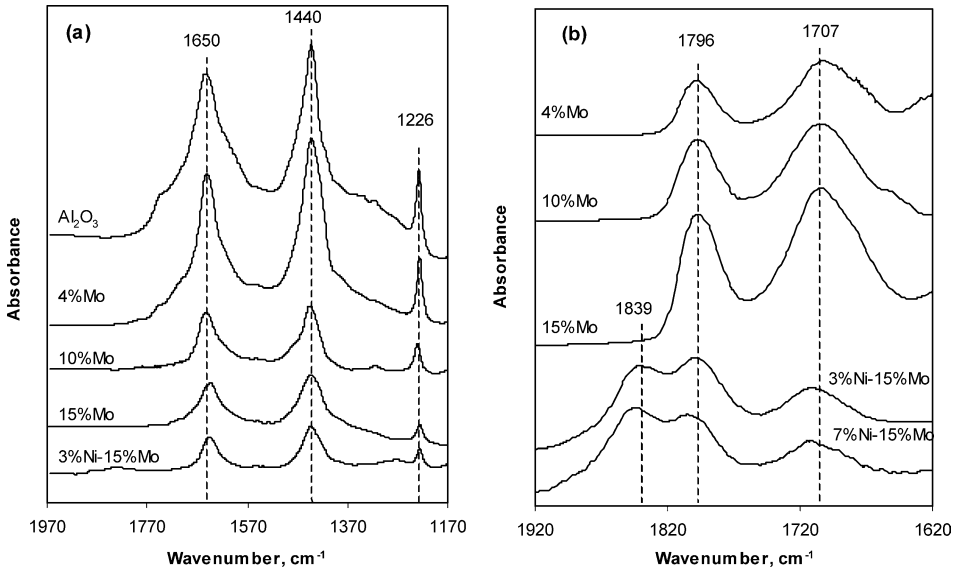

Fig. 1. DRIFTS spectra of CO_2 and NO adsorbed on sulfided samples. (a) CO_2 spectra, (b) NO spectra.

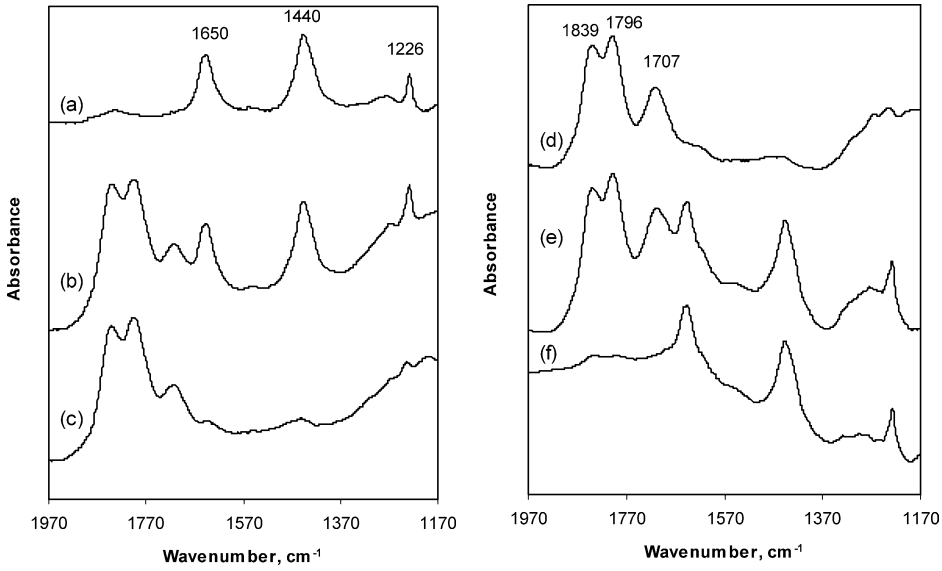

Fig. 2. DRIFTS spectra of adsorbed CO_2 and NO on sulfided bimetallic 3% Ni–15% Mo/Al_2O_3 catalyst. (a) CO_2 adsorption at RT, (b) NO adsorption at RT after a, (c) subtraction of a from b, (d) NO adsorption at RT, (e) CO_2 adsorption at RT after d, (f) subtraction of d from e.

exhibits an additional band at 1839 cm^{-1}, which is associated with Ni sites. The intensity of this band increases with increasing Ni loading. Also noted in these spectra is that the intensity of Mo-associated bands decreases with increasing Ni loading, suggesting that some of the surface Mo centers are being "replaced" or taken up by Ni sites.

Fig. 2 shows consecutive adsorption of CO_2 (a) followed by NO (b) over sulfided Ni–Mo catalyst. Spectra taken after CO_2 followed by NO adsorption exhibit bands that were seen in individual NO and CO_2 adsorption experiments. Fig. 2c shows the spectrum that was the result of subtraction of a from b. The resulting spectrum in identical to the spectrum obtained when only NO is adsorbed on the surface (d), indicating that there is minimal interference between the CO_2 and the NO adsorption sites. The spectrum taken after consecutive adsorption of NO and CO_2 is identical to the spectrum taken where the order of adsorption was reversed (e). Fig. 2f shows the difference spectrum obtained when e was subtracted from d. This spectrum is identical to the one obtained following CO_2 adsorption only (a), except for the base line shift, reiterating the earlier findings that the CO_2 and NO adsorb on distinct sites which are essentially independent of each other. A similar observation was reported earlier for a monometallic Mo/Al_2O_3 catalyst [15].

The IR spectra of the hydroxyl regions of calcined and sulfided catalysts are shown in Fig. 3. The deconvolution of the bands representing the OH groups (3675, 3728, 3769, and 3778 cm^{-1}) and the chemisorbed wa-

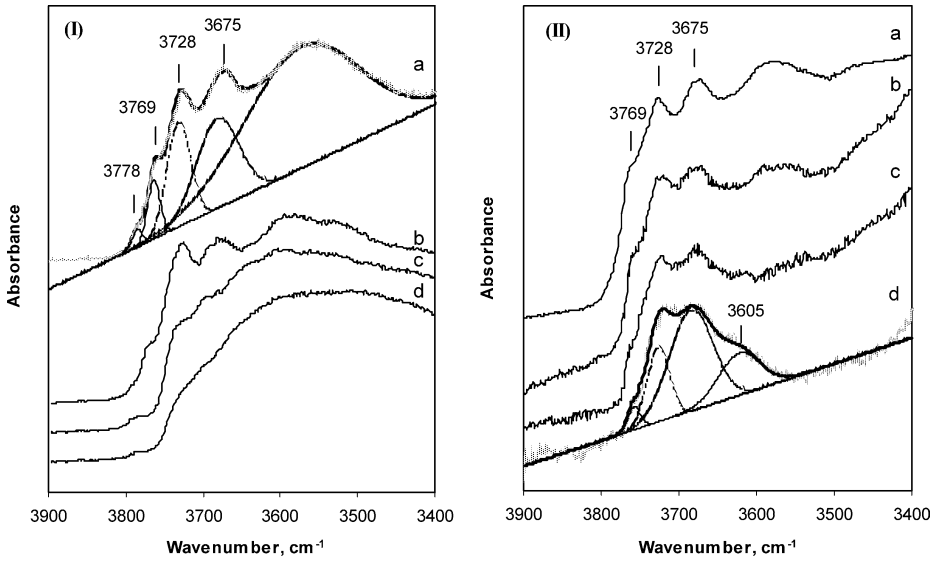

Fig. 3. Hydroxyl region of IR spectra for oxidic (I) and sulfided (II) γ-Al_2O_3 and Mo/Al_2O_3 samples. (a) Al_2O_3, (b) 4% Mo/Al_2O_3, (c) 10% Mo/Al_2O_3, (d) 15% Mo/Al_2O_3.

ter (3580–3600 cm^{-1}) over the calcined alumina surface is shown in Fig. 3I, a. As reported previously in the literature [18,23–28], the intensity of the OH bands decrease with increasing Mo loading, as molybdena species "anchor" onto the OH groups on the alumina surface. The band positions for OH groups on sulfided Al_2O_3 support are not any different from those on oxidic Al_2O_3 support. The decrease of the intensity of OH bands with increasing Mo loading is less pronounced over the sulfided catalysts compared to the oxide samples. Another difference between the oxide and the sulfide samples is that the intensity of chemisorbed water band (3580–3600 cm^{-1}) decreases with increasing MoO_3 loading, while a broad band centered around 3605 cm^{-1} grows gradually. This band has been attributed to H bonding associated with SH groups over the sulfided catalysts and has been referred to as an indirect evidence of the presence of sulfhydryl groups on MoS_2 slabs [29,30]. The OH absorbances for the 3675, 3728, and 3769 cm^{-1} bands normalized with respect to those found over the bare alumina support are plotted against MoO_3 loading (Fig. 4). The solid lines represent the calcined catalysts whereas the dashed lines denote the sulfided catalysts. The OH groups over the sulfide samples have higher relative absorbance than the oxide samples. For both oxide and sulfide catalysts, the normalized intensities of all OH bands decrease with Mo loading up to 15%, after which there is no significant change. Another point to note is that the intensity of the band at 3769 cm^{-1} decreases faster with MoO_3 loading, compared to the intensity of the 3728 and 3675 cm^{-1} bands. This difference, which is seen in both oxide and sulfide samples, is especially noticeable at the lower loading levels. This indicates a higher affinity of Mo species toward the more basic OH groups on the surface. A similar observation was reported earlier for oxide samples [30], although the authors did not observe the same trend for the sulfided samples. The data points from

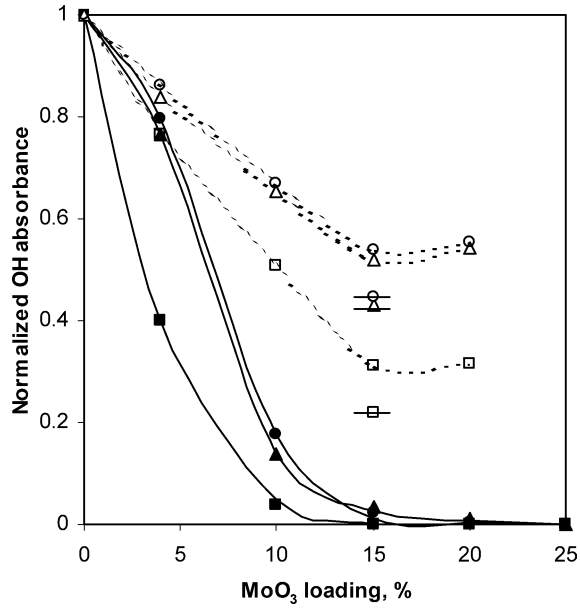

Fig. 4. Normalized OH band absorbance vs MoO_3 loading for calcined (filled symbols) and sulfided (blank symbols) catalysts. (● ○), (▲ △), and (■ □) represent the 3675, 3728, and 3769 cm^{-1} bands, respectively. (⊖ ⧋ ⊟) represent the data points for sulfided 3% Ni–15% Mo/Al_2O_3 catalysts.

sulfided 3% Ni–15% Mo/Al_2O_3 bimetallic catalyst are also included in Fig. 4. It can be seen that the normalized intensities for all OH bands from sulfided 3% Ni–15% Mo/Al_2O_3 bimetallic catalysts are significantly lower than those of the sulfided 15% Mo/Al_2O_3 monometallic catalysts. This observation is consistent with earlier finding about the effect of Ni to enhance the Mo dispersion [19].

Fig. 5 shows IR spectra of the hydroxyl region of the sulfided γ-Al_2O_3 and sulfided Mo/Al_2O_3 catalysts after CO_2 adsorption. The background spectrum obtained prior to CO_2 chemisorption is subtracted from each spectrum. The band

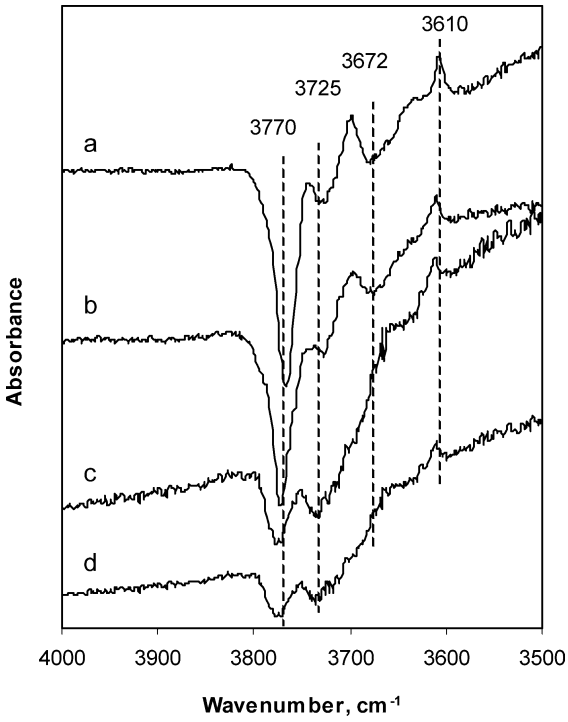

Fig. 5. Hydroxyl region of IR spectra for sulfided samples after CO_2 adsorption. (a) Al_2O_3, (b) 4% Mo/Al_2O_3, (c) 10% Mo/Al_2O_3, and (d) 15% Mo/Al_2O_3.

at 3610 cm^{-1} is attributed to the OH stretching mode of bicarbonate species adsorbed on γ-Al_2O_3 [13,20]. The negative peaks seen in the difference spectra show that the depletion of the more basic OH groups represented by the high-frequency bands (3760–3780 cm^{-1}) is much more pronounced compared to the other hydroxyl groups. The negative peaks associated with the depletion of other OH groups are much less noticeable. This suggests that CO_2 has higher affinity for the more basic OH groups and it does not indiscriminately "titrate" all of the OH groups. When we combine this observation with our earlier findings that the molybdena species also interact preferentially with more basic hydroxyl groups (Fig. 4), one can see that using CO_2 chemisorption will lead to a higher estimate of the surface coverage. As pointed out by Topsoe and co-workers [29], it appears that the CO_2 adsorption method is likely to provide much better estimations for surface coverage over the sulfide catalysts than over the oxidic samples. The trends seen in Fig. 4 are in agreement with this assertion.

3.2. Volumetric measurements of NO and CO_2 chemisorption

CO_2 chemisorption is frequently used to monitor the free alumina surface and provide information about the coverage of alumina support [13,15–17]. It has also been applied to Mo/TiO_2 catalysts [31,32]. The amount of chemisorbed CO_2 measured volumetrically and the surface coverage calculated with Eq. (1) are plotted in Fig. 6 as a function of MoO_3 loading. Consistent with our DRIFTS results and as reported earlier in the literature [33], the CO_2 chemisorption on oxidic samples decreases sharply with the first small increase in metal loading. The corresponding coverage increases similarly at lower MoO_3 loading, presenting a nonlinear correlation with the MoO_3 loading. As discussed above and also concluded in the literature [29,33], since CO_2 does not fully titrate all of the surface OH groups, the coverage estimated by this method is expected to be higher than actual. For the sulfide catalysts, the amount of CO_2 adsorbed is higher than it is for the oxide. The coverage estimated follows a somewhat linear trend up to 15% Mo loading. When similar calculations are performed as a function of Ni loading on bimetallic catalysts where Mo loading is kept constant, the effect of Ni loading on CO_2 adsorption and surface coverage is found to be negligible.

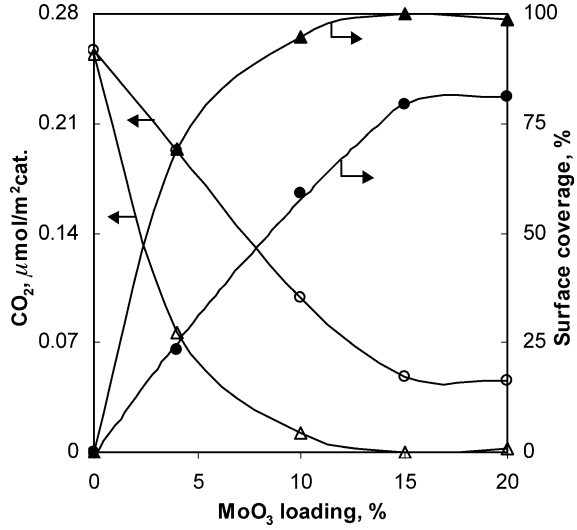

Fig. 6. CO_2 chemisorption (blank symbols) and surface coverage (filled symbols) calculated based on CO_2 adsorption over oxidic (▲, △) and sulfided (●, ○) Mo/Al_2O_3 samples.

It appears that a quantification of surface OH groups would provide a better estimate of the exposed alumina surface than CO_2 adsorption measurements. The surface coverage of Al_2O_3 support, Cs_{OH}, based on the total absorbance of OH groups normalized with respect to the bare alumina surface, was calculated by the expression

$$\%Cs_{OH} = \left[1 - \left\{A_{cat}/(1 - m/100)\right\}/A_{Al}\right] \times 100, \qquad (2)$$

where A_{cat} and A_{Al} are the sum of the absorbance of free OH groups on catalysts and on Al_2O_3 support, respectively. m is the wt% of MoO_3 loading in the oxidic catalysts. Fig. 7 shows the surface coverage as a function of MoO_3 loading calculated with Eq. (2) for both oxidic and sulfided catalysts. Comparing Fig. 7 with Fig. 6, the surface coverage obtained from the relative intensity of OH bands is lower than that calculated from CO_2 chemisorption for both oxidic and sulfided catalysts. Here the decreases in OH band intensities are due to consumption of OH groups by Mo species. In Fig. 7, it can be seen that, for oxidic catalysts, the surface cover-

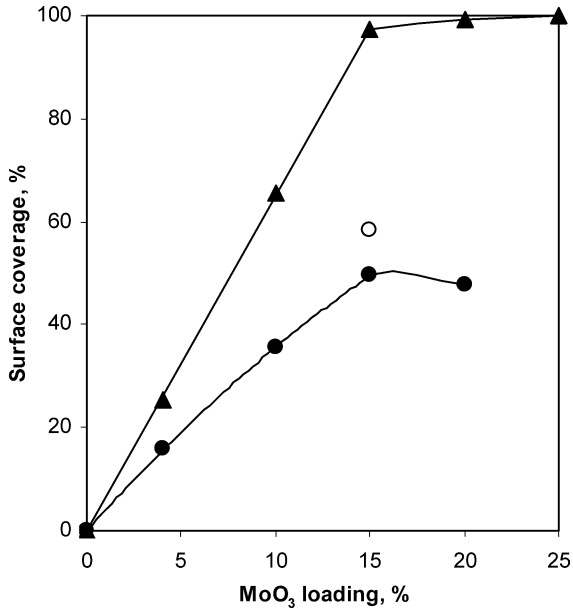

Fig. 7. Surface coverage of Al_2O_3 calculated from relative intensities of OH bands as a function of MoO_3 loading. ▲—oxidic and ●—sulfided Mo/Al_2O_3 catalysts. Blank point represents sulfided 3% Ni–15% Mo/Al_2O_3 catalyst.

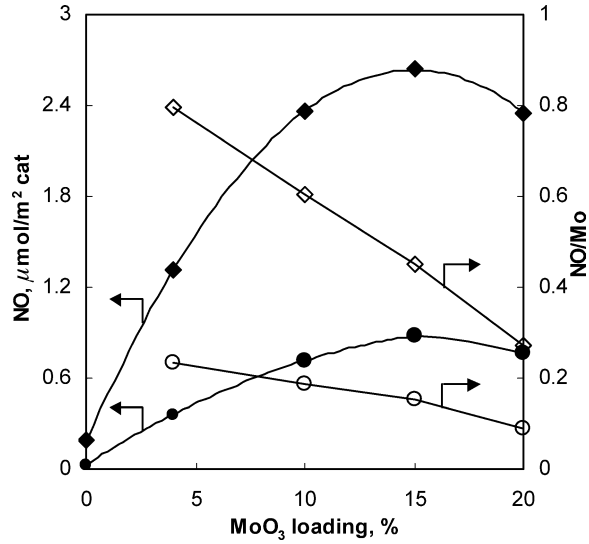

Fig. 8. NO chemisorption and NO/Mo ratio as a function of MoO_3 loading for sulfided Mo/Al_2O_3 catalysts. (●, ○) Adsorption at 30 °C; (◇, ◆) adsorption at −78 °C. Filled and blank symbols represent NO adsorption and NO/Mo ratio, respectively.

age increases linearly to almost 100% with increasing MoO_3 loading up to 15%. It is clear that below 15% loading, MoO_3 disperses on Al_2O_3 to form a monolayer. Additional MoO_3 loading leads to formation of three-dimensional structures on Al_2O_3 surface, as identified by XRD [20]. The surface coverage decreases after sulfidation for all catalysts with different MoO_3 loading. Over the oxide surfaces Mo species bond to OH groups, achieving a high dispersion over the alumina surface up to loading levels of 15% or higher. During the sulfidation process, Mo–O–Al bonds are broken and Mo agglomerates to form small MoS_2 slabs on the alumina support. The EXAFS results [34] showed that Mo in the calcined sample is present in highly disordered structures, whereas the sulfided catalysts contain MoS_2-like domains, which are ordered. This explains the lower surface coverage observed over the sulfided catalysts. The variation of surface coverage with loading, however, is not exactly linear and shows a downward curvature, suggesting that with increasing loading, the thickness of the MoS_2 slabs may be growing, although the surface is not fully covered. As seen in DRIFTS and CO_2 adsorption results, the bimetallic catalyst shows a higher surface coverage than the monometallic catalyst at the same loading level.

NO is one of the most frequently used molecules for characterizing hydrotreating catalysts. It is widely accepted that it can be used to probe the anion vacancies (i.e., coordinatively unsaturated sites) over Ni–Mo–S and Co–Mo–S systems. Fig. 8 shows NO chemisorption amount at 30 and −78 °C as a function of MoO_3 loading for sulfided MoO_3/Al_2O_3 catalysts. The results are in agreement with those reported earlier by Massoth and co-workers [35], that NO adsorption on sulfided catalysts decreases over both the catalyst and the support with increasing adsorption temperature. NO, being an oxidant [36,37], may oxidize the surface of the sulfided or reduced catalyst, especially in a static analysis system where the contact time may be long. N_2O and N_2 have been detected as desorption products of NO adsorption studies of reduced MoO_3/Al_2O_3 catalysts [38]. It was also pointed out that no oxidation reactions were observed when NO was adsorbed at a temperature of −78 °C. As expected, the amount of NO adsorbed at −78 °C was much higher than the amount adsorbed at 30 °C. In correlating the NO adsorption sites with reaction data, the results obtained at −78 °C were used. For both temperatures at which NO chemisorption data are collected, the NO adsorbed increases sharply with increasing Mo loading level up to 15% MoO_3, showing a direct correlation of CUS sites with molybdenum. Further increase in Mo loading causes a decrease in NO adsorption capacity since additional Mo leads to the formation of crystalline MoO_3 in the oxide phase, which is sulfided to form crystalline MoS_2 particles on the surface. It should be noted that the NO uptake over the bare alumina surface is not exactly zero at −78 °C, although it is very close to zero at 30 °C. This could be due to some oxygen vacancies remaining on the support. The other point to note about the NO adsorption results is that the Ni addition increases the NO uptake capacity, agreeing with earlier assertions about the formation of CUS sites associated with Ni centers [19]. Also shown in the same figure is the variation of NO/Mo ratio with Mo loading which shows a negative slope. As the loading level increases, the additional Mo may either increase the number of slabs or cause the slabs to grow. Since NO adsorption is related to the edge sites of the slabs, the adsorbed amount of NO should be proportional to the MoO_3 loading, if the same size of slabs is maintained and only the number of slabs increases. The decrease in the

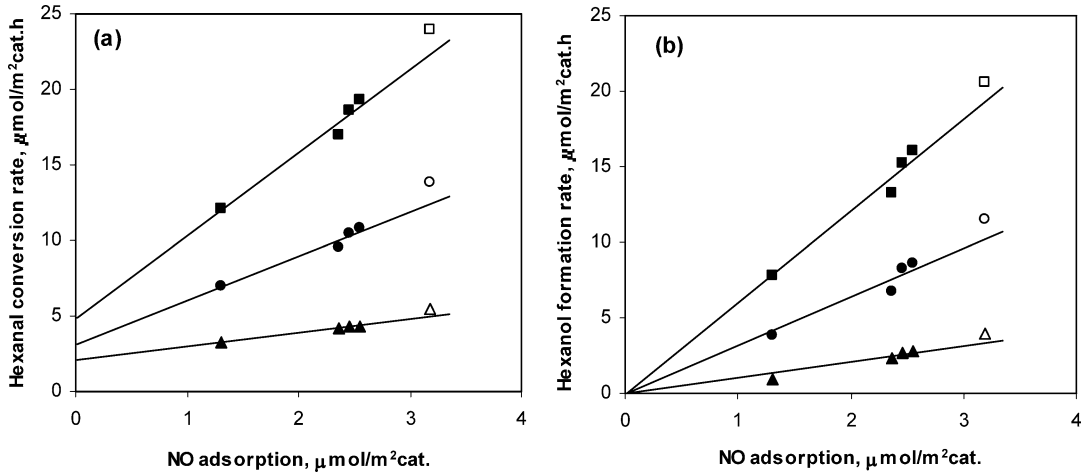

Fig. 9. Hexanal conversion rate (a) and hexanol formation rate (b) in hexanal hydrogenation over sulfided catalysts as a function of NO chemisorption. (■) 180 °C, (●) 160 °C, (▲) 140 °C. Blank symbols represent the data from sulfided bimetallic 3% Ni–15% Mo/Al_2O_3 catalyst.

NO/Mo ratio with increasing MoO_3 loading shows that the slab size also increases. This result, which is in agreement with that reported by Cacers et al. [39], is somewhat different from that reported by Miciukiewicz et al. [35], who have shown a linear correlation of NO adsorption (at 0 °C) with Mo loading, measured with pulse techniques and corrected with surface coverage calculated from CO_2 chemisorption, with Mo loading up to 8%. Their conclusion was that the same slab size was maintained and only the number of slabs increased with increasing Mo level. It is conceivable that at lower loading levels additional Mo increases the number and density of the MoS_2 slabs on the surface without causing any growth of the slabs themselves.

3.3. Correlations of adsorption sites with aldehyde hydrogenation performance

As reported previously [20,21], the CUS sites or anion vacancies are proposed to be the active sites for hydrogenation of aldehyde, while the OH groups on exposed Al_2O_3 surface appear to be responsible for promoting the side reactions that produce heavy products. In the following sections, we present the correlations of adsorption sites with hydrogenation performance in an effort to account for the trends that we see in activity and selectivity of these catalysts. It was reported [40–42] that the extent of NO chemisorption seemed to correlate better with catalytic activity than O_2 adsorption due to the fact that NO chemisorption is more selective than that of O_2. The drawbacks of the use of NO as a probe molecule for hydrotreating catalysts include the possibility of catalyst surface oxidation by NO and adsorption amount being a function of temperature. Oxidation of the surface with NO can be avoided by selecting lower adsorption temperatures (−78 °C) [38]. Although it may not be possible to obtain the absolute number of sites with NO adsorption, under a fixed set of experimental conditions, it is reasonable to assume that the same fraction of adsorption sites is being measured, as suggested by Massoth and co-workers [35]. The following correlations were performed under constant conditions and at −78 °C.

3.3.1. Hexanal hydrogenation

The variation of hexanal conversion rate and hexanol formation rate with NO uptake at −78 °C is shown in Fig. 9. In the experimental temperature range of 140 to 180 °C, hexanal conversion rate appears to correlate linearly with NO uptake at −78 °C (Fig. 9a). Each point corresponds to a different catalyst. The linear correlation suggests that the active sites for hexanal hydrogenation are the same sites for NO adsorption, which are the anion vacancies (CUS), the generally accepted active sites for hydrogenation in the hydro-treating literature. One interesting observation about the data is that, when the lines are extrapolated to zero NO uptake, hexanal conversion rates do not go through the origin. Since the correlation is for the overall hexanal conversion, it appears that there are side reactions of hexanal, which do not require hydrogenation sites. Our studies, which focused on the reaction pathways of aldehyde hydrogenation [21], have shown the bare Al_2O_3 support to have a high activity for the condensation-type reactions of aldehyde itself to form heavy products. Therefore, it is expected for the overall hexanal conversion rate not to go to zero when the NO uptake is extrapolated to zero. Fig. 9b, which shows the correlation of hexanol formation rate with NO uptake, supports this assertion. The variation of hexanol formation rate with NO uptake is linear, and the extrapolated lines go through the origin. This implies that the coordinatively unsaturated sites are indeed the active site for hexanal hydrogenation to form hexanol. The blank symbols in Fig. 9 represent the hexanal conversion rate and hexanol formation rate on sulfided 3% Ni–15% Mo/Al_2O_3 bimetallic catalyst, respectively. For all three temperatures, the data points for the bimetallic catalysts fall on or slightly above the straight lines. The number of NO adsorption experiments conducted with bimetallic catalysts is not large enough to make this assertion, however, one might expect the activity to be higher

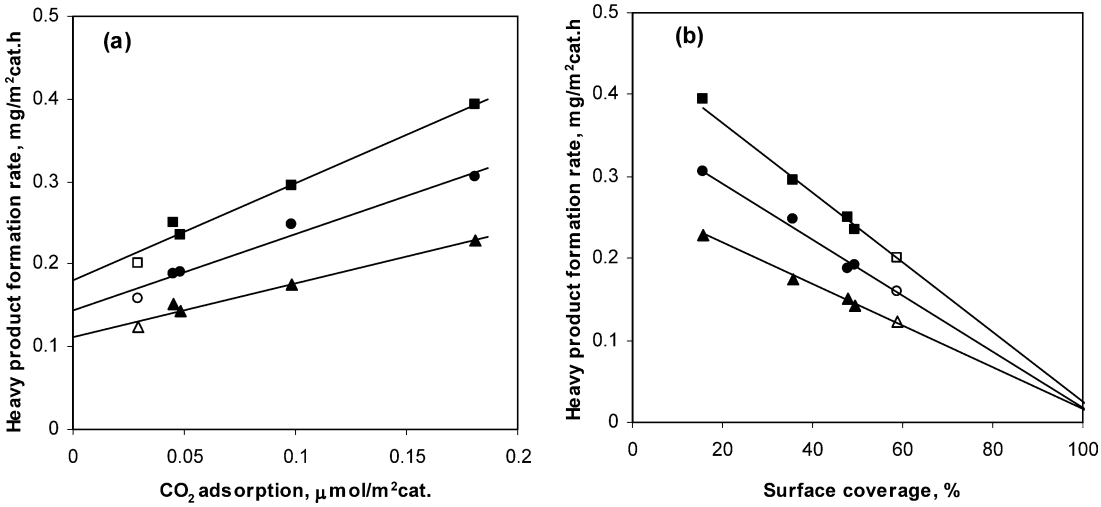

Fig. 10. Heavy product formation rate in hexanal hydrogenation over sulfided catalysts as a function of (a) CO_2 chemisorption, (b) surface coverage based on relative intensities of OH bands. (■) 180 °C, (●) 160 °C, (▲) 140 °C. Blank symbols represent the data from sulfided bimetallic 3% Ni–15% Mo/Al_2O_3 catalyst.

(and hence the bimetallic catalyst data points to fall somewhat above the straight line) based on earlier reports in the literature, where Ni-associated S vacancies in the Ni–Mo–S phase were shown to have a higher intrinsic activity than the Mo-associated S vacancies [12,19,43].

Fig. 10 shows the heavy product formation rates plotted against CO_2 uptake obtained from volumetric chemisorption experiments and alumina surface coverage obtained from total consumption of OH groups on the catalysts. The filled symbols represent different catalyst compositions among the monometallic Mo catalysts. The heavy product formation rate increases linearly with increasing CO_2 uptake (Fig. 10a), suggesting a correlation between the CO_2 adsorption sites and the active sites for the heavy product formation. However, the extrapolated lines do not go through the origin. As indicated earlier, CO_2 uptake provides some measure of the exposed alumina surface. However, a better measurement is the depletion of the OH groups on the surface. When the heavy product formation rate is plotted against the surface coverage calculated using the IR absorption intensity of the OH bands (Fig. 10b), again a linear correlation appears. The points representing the data from bimetallic catalysts also fall on these lines. It appears that the surface hydroxyl groups on the exposed alumina surfaces are the main sites for the condensation-type reactions.

Although the heavy product formation rate correlates better with concentration of the surface hydroxyl groups, the rate does not drop to zero when surface coverage is 100% (i.e., OH groups on the alumina surface are completely depleted). It is conceivable that the sulfhydryl (SH) groups found on the MoS_2 slabs could be contributing to the heavy product formation activity. This possibility is supported by several reports in the literature, which attribute hydrogenolysis activity to the Brønsted acid sites associated with SH groups [43–50]. Some correlations between the HDS activity and the estimated SH concentration have been reported for promoted [44,51–53] and unpromoted catalysts [35], including some studies that probed the Brønsted acid sites using pyridine adsorption [29]. Since most of the heavy products observed require an initial dehydration step, active sites that promote the cleavage of C-heteroatom bonds could also contribute to the formation of the heavy product formation by catalyzing this initial step.

3.3.2. *Propanal hydrogenation*

Fig. 11 shows the propanal conversion rates and propanol formation rates at two different feed concentrations plotted as a function of NO uptake at −78 °C. Similar to the trends observed for hexanal, propanal conversion rates decrease with the decreasing NO uptake. The extrapolated lines for propanal conversion do not go through the origin, showing that the catalysts would still have significant propanal conversion activity even when there are no more NO chemisorption sites. It also appears that the smaller aldehyde has a higher reactivity over the bare alumina surface than the larger one. Another comparison one can make between the two aldehydes is that propanol formation rate reaches zero even when there are NO adsorption sites on the surface. Results obtained by using alcohols (propanol and hexanol) as feed molecules showed a higher reactivity for propanol, suggesting that the "observed" formation rate of propanol may be significantly lower than the actual formation rate due to further reaction of propanol once it is formed [21]. This would explain the minus formation rates for propanol when NO adsorption is extrapolated to zero.

Fig. 12 demonstrates the correlations of heavy product formation rates with CO_2 uptake and with alumina surface coverage obtained from the IR data for the OH groups, using two different feed concentrations. The trends are similar to those obtained for hexanal hydrogenation presented

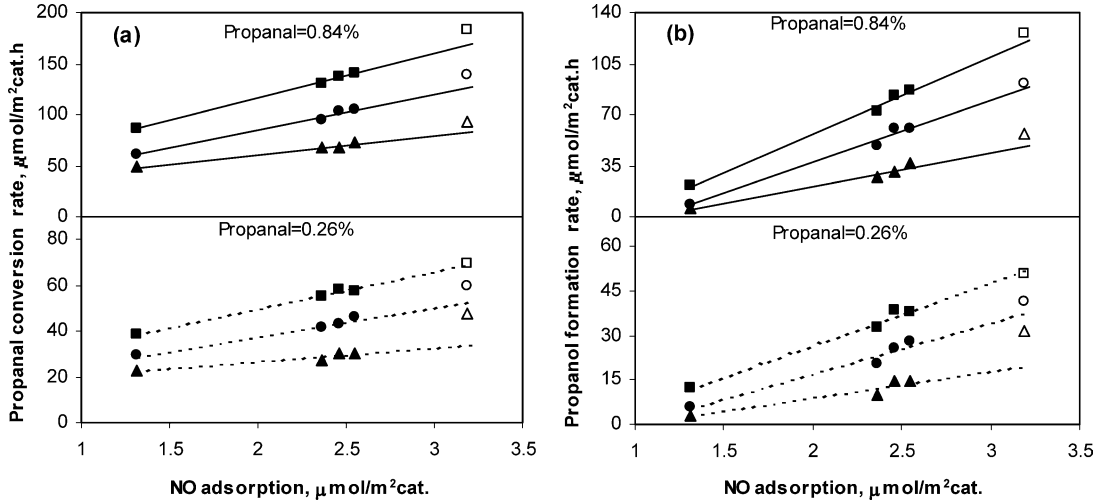

Fig. 11. Propanal conversion rate (a) and propanol formation rate (b) in propanal hydrogenation over sulfided catalysts as a function of NO chemisorption. (■) 180 °C, (●) 160 °C, (▲) 140 °C. Blank symbols represent the data from sulfided bimetallic 3% Ni–15% Mo/Al_2O_3 catalyst.

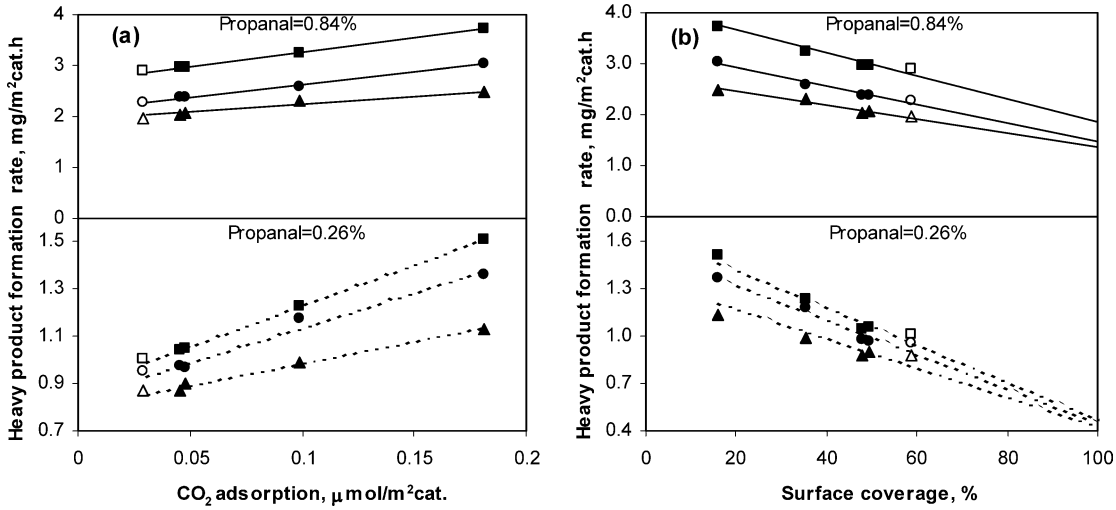

Fig. 12. Heavy product formation rate in propanal hydrogenation over sulfided catalysts as a function of (a) CO_2 chemisorption, (b) surface coverage based on relative intensities of OH bands. (■) 180 °C, (●) 160 °C, (▲) 140 °C. Blank symbols represent the data from sulfided bimetallic 3% Ni–15% Mo/Al_2O_3 catalyst.

in Fig. 10. However, the heavy product formation rates per catalyst surface area are much higher for propanal hydrogenation than they are for hexanal hydrogenation, which is consistent with the observation discussed above.

4. Summary

NO adsorption and CO_2 adsorption measurements, which are used to probe the coordinatively unsaturated sites and the hydroxyl groups on the alumina surface, were found to correlate well with alcohol and heavy product formation rates, respectively. The anion vacancies associated with Ni sites were found to have a higher intrinsic activity for hydrogenation of aldehyde to alcohol. Although CO_2 can provide some measure of the exposed alumina surface, it tends to overestimate the surface coverage since it adsorbs preferentially on more basic OH sites. Therefore, quantification of the OH groups relative to the bare alumina surface appears to provide a more accurate measure of the surface coverage. As reported previously, the sulfided catalyst were found to have more alumina surface exposed compared to the oxidic samples due to Mo aggregation during the formation of the MoS_2 slabs. It appears that the OH groups on alumina surface are the primary sites leading to heavy product formation through condensation-type reactions. It is also conceivable that Brønsted acid sites associated with SH groups may be contributing to these reactions. The trends observed for the two different linear aldehydes used as feed molecules were quite similar.

In the next article of this series, the effect of postsulfidation treatment conditions on the aldehyde hydrogenation performance of the NiMoS catalysts will be presented.

References

[1] G.C.A. Schuit, B.C. Gates, AIChE J. 19 (1973) 417.
[2] P. Grange, Catal. Rev.-Sci. Eng. 21 (1980) 135.
[3] H. Topsoe, B.S. Clausen, Catal. Rev.-Sci. Eng. 26 (1984) 395.
[4] R. Prins, V.H.J. de Beer, G.A. Somorjai, Catal. Rev.-Sci. Eng. 31 (1989) 1.
[5] R.R. Chianelli, M. Daage, M.J. Ledoux, Adv. Catal. 40 (1994) 177.
[6] H. Topsoe, B.S. Clausen, F. Massoth, in: J.R. Anderson, M. Boudart (Eds.), Hydrotreating Catalysis, Science and Technology, vol. 11, Springer, Berlin, 1996.
[7] D.D. Whitehurst, T. Isoda, I. Mochida, Adv. Catal. 42 (1998) 345.
[8] H. Topsoe, B.S. Clausen, R. Candia, C. Wivel, S. Morup, J. Catal. 68 (1981) 433.
[9] C. Wivel, R. Candia, B.S. Clausen, S. Morup, H. Topsoe, J. Catal. 87 (1984) 497.
[10] H. Topsoe, B.S. Clausen, Appl. Catal. 25 (1986) 273.
[11] J.J. MeKetta, W.A. Cunningham (Eds.), Encyclopedia of Chemical Processing and Design, vol. 33, 1990, p. 46, New York.
[12] L. Portela, P. Grange, B. Delmon, Catal. Rev.-Sci. Eng. 37 (4) (1995) 699.
[13] K. Segawa, W.K. Hall, J. Catal. 77 (1982) 221.
[14] J. Valyon, R. Schneider, W.K. Hall, J. Catal. 85 (1984) 277.
[15] W.S. Millman, K. Segawa, D. Smrz, W.K. Hall, Polyhedron 5 (1986) 169.
[16] W. Zmierczak, Q. Qader, F.E. Massoth, J. Catal. 106 (1987) 65.
[17] C. O'young, C. Yang, S.J. DeCanio, M.S. Patel, D.A. Storm, J. Catal. 113 (1988) 307.
[18] U.S. Ozkan, S. Ni, L. Zhang, E. Moctezuma, Energy Fuels 8 (1994) 249.
[19] U.S. Ozkan, L. Zhang, S. Ni, E. Moctezuma, J. Catal. 148 (1994) 181.
[20] X. Wang, G. Li, U.S. Ozkan, J. Mol. Catal. 217 (2004) 219.
[21] X. Wang, R.Y. Saleh, U.S. Ozkan, to be submitted.
[22] A.M. Turek, I.E. Wachs, E. DeCanio, J. Phys. Chem. 96 (1992) 5001.
[23] J.M.J.G. Lipsch, G.A. Schuit, J. Catal. 15 (1969).
[24] P. Ratnasamy, A.V. Ramaswamy, K. Banerjee, D.K. Sharma, N. Ray, J. Catal. 38 (1975) 19.
[25] T. Fransen, O. Van der Meer, P. Mars, J. Catal. 42 (1976) 79.
[26] P. Ratnasamy, H. Knozinger, J. Catal. 54 (1978) 155.
[27] N. Topsoe, J. Catal. 64 (1980) 235.
[28] Y. Okamoto, T. Imanaka, J. Phys. Chem. 92 (1988) 7102.
[29] N.-Y. Topsoe, H. Topsoe, J. Catal. 119 (1989) 252.
[30] N.-Y. Topsoe, H. Topsoe, J. Catal. 139 (1993) 631.
[31] K. Segawa, D.S. Kim, Y. Kurusu, I.E. Wachs, in: M.J. Phillips, M. Ternan (Eds.), Proc., 9th Int. Congress on Catalysis, Calgary, 1988, The Chemical Institute of Canada, Ottawa, 1988, p. 1960.
[32] S. Rondon, M. Houalla, D.H. Hercules, Surf. Interface Anal. 26 (1998) 329.
[33] F.M. Mulcahy, K.D. Kozminski, J.M. Slike, F. Ciccone, S.J. Scierka, M.A. Eberhardt, M. Houalla, D.M. Hercules, J. Catal. 139 (1993) 688.
[34] B.S. Clausen, H. Topose, R. Candla, J. Villladsen, J. Phys. Chem. 85 (1981) 3868.
[35] J. Miciukiewicz, W. Zmierczak, F.E. Massoth, Bull. Soc. Chim. 96 (1987) 915.
[36] A. Kazusaka, R.F. Howe, J. Catal. 63 (1980) 447.
[37] Z. Shusian, W.K. Hall, G. Ertl, H. Knozinger, J. Catal. 100 (1986) 167.
[38] A. Redey, J. Goldwasser, W.K. Hall, J. Catal. 113 (1988) 82.
[39] C.V. Cacers, J.L.G. Fierro, A.L. Agudo, M.N. Blanco, H.J. Thomas, J. Catal. 95 (1985) 501.
[40] H.J. Jung, J.L. Smitt, H. Ando, in: H.F. Barry, P.C.H. Mitchell (Eds.), Proc., 4th Conf. Chemistry and Uses of Molybdenum, Climax Molybdenum, Ann Arbor, MI, 1982, p. 246.
[41] N. Topose, H. Topose, J. Catal. 75 (1982) 354.
[42] A.L. Agudo, F.J.G. Llambias, J.H.D. Tascon, J.L.G. Fierro, Bull. Soc. Chim. Belg. 93 (1984) 719.
[43] L. Zhang, G. Karakas, U.S. Ozkan, J. Catal. 178 (1998) 457.
[44] J. Maternova, Appl. Catal. 3 (1982) 3.
[45] S.H. Yang, C.N. Satterfield, J. Catal. 81 (1983) 168.
[46] J. Maternova, Appl. Catal. 6 (1982) 61.
[47] G. Muralidhar, F.E. Massoth, J. Shabtai, J. Catal. 85 (1984) 44.
[48] A.Y. Bunch, U.S. Ozkan, J. Catal. 206 (2002) 177.
[49] A.M. Escudey-Castro, L.B. McLeeod, E.J. Gil-Llambias, Appl. Catal. 4 (1982) 371.
[50] F.E. Massoth, in: Proc., 4th Int. Conf., Chemistry and Uses of Molybdenum, Golden, CO, 1982.
[51] X. Wang, U.S. Ozkan, submitted for publication.
[52] V. Stuchly, L. Baranek, Appl. Catal. 35 (1987).
[53] L. Vivier, Kasztelan, G. Perot, Bull. Soc. Chim. Belg. 100 (1991) 801.